8. H. G. Maas, A high-resolution photogrammetric 3-D particle tracking velocimeter, *Experimental and Numerical Flow Visualization ASME FED*, Vol. 128, 79-84, (1991);
9. B.B. Mandelbrot and Van Ness J.W., Fractional Brownian Motion, Fractional Noises and Applications, *SIAM Rev*, 10, 422-437, (1968);
10. B.B. Mandelbrot, Les Objects Fractals: Forme, Hasard et Dimension. Flammarion, Paris, (1975);
11. B.B. Mandelbrot, The fractal geometry of Nature, Freeman, San Francisco, (1982);
12. M. Matsushita and S. Ouchi, On the Self-Affinity of Various Curves, *Phisica*, No. 38, (1989);
13. H.O. Peitgen and D. Saupe, The Science of Fractal Images, Springer, Berlin, (1988);
14. R. G. Racca and J. M. Dewey, A method for automatic particle tracking in a three-dimensional flow field, *Experiments in Fluids 6*, 25-32, (1988);
15. P. G. Saffman, On the effect of the molecular diffusivity in turbulent diffusion, *J. Fluid Mech.* 8, 273-283 (1959);
16. S. Saleh, J. F. Thovert and P. M. Adler, Etude des milieux poreux par P.I.D.V., *2ème Congrès Francophone de Velocimétrie Laser*, Lab. d'Aerothermique du CNRS, Meudon, (1990);
17. S. Saleh, J. F. Thovert and P. M. Adler, Flow along porous media by Particle Image Velocimetry, *AIChE Journal*, 39 (11), 1765-1776 (1993);
18. S. Saleh, J. F. Thovert and P. M. Adler, Measurement of two-dimensional velocity fields in porous media by particle image displacement velocimetry, *Experiments in Fluids 12*, 210-212 (1992);
19. P. Viotti, Scaling properties of tracer trajectories in a saturated porous medium, accepted for *Transport in porous media*, (1996);
20. R.F. Voss, The Science of Fractal Images, H.O. *Peitgen and D.Saupe eds. Springer*, Berlin, (1988);
21. S.W. Wheatcraft and S.W. Tyler, An Explanation of Scale-dependent Dispersivity in Heterogeneous Aquifers Using Conceps of Fractal Geometry, *Water Resources Res.* 24(4), 566-578, (1988).

SCALING GYROSCOPES CASCADE: UNIVERSAL MULTIFRACTAL FEATURES OF 2-D AND 3-D TURBULENCE

Y. CHIGIRINSKAYA , D. SCHERTZER
Laboratoire de Météorologie Dynamique, Université Pierre et Marie Curie, Paris, France

S. LOVEJOY
Physics Department, McGill University, Montreal, Canada

Similarities between the structure of the Navier-Stokes equations of hydrodynamic turbulence and the Euler equations of a gyroscope lead to the consideration of a dynamical space-time model, the Scaling Gyroscopes Cascade (SGC), built up on a certain type of direct interaction closely respecting this analogy. With the help of this model we investigate the multifractal features of intermittency of the direct energy cascade in three-dimensional turbulence, and of the inverse energy cascade in the two-dimensional turbulence. We obtain rather similar universal multifractal parameters for both cases, whereas the shell-model which is obtained by an over-simplification of the SGC yields quite different estimates.

1 Introduction

Similarities [1,2] between the Navier-Stokes equations of hydrodynamic turbulence and the Euler equations of a gyroscope can be traced back to Lamb [3]. However, we show that for three-dimensional (3-D) turbulence as well as for two-dimensional (2-D) turbulence, direct interactions between eddies yield much closer analogies than previously considered. The corresponding non-direct interactions are obtained by coupling an infinite hierarchy of gyroscopes. This yields a dynamical space-time cascade [4], the Scaling Gyroscopes Cascade (SGC) which should preserve most of the properties of the Navier-Stokes equations.

The respective analogies for 2-D and 3-D are rather opposite: the analogue of the angular momentum of a solid body rotation is the vorticity field for 2-D turbulence, whereas it is the velocity field for 3-D turbulence. However, the multifractal characteristics of the inverse energy cascade sub-range of the former are extremely close to those of the direct energy cascade of latter. We also find a surprisingly close agreement with various empirical studies on atmospheric turbulence. It is important to note that the SGC yields the direct enstrophy cascade for the 2-D turbulence as well as the inverse energy cascade.

2 A first aspect of similarity between hydrodynamic turbulence and gyroscopes

Consider the Navier-Stokes equations, for the velocity field $\underline{u}(\underline{x},t)$, written under Bernoulli's form (α being the kinematic pressure, i.e. for barotropic flows: $\alpha = \int \frac{dp}{\rho(p)} + \frac{u^2}{2}$, p being the (static) pressure; ν is the fluid viscosity):

$$\left(\frac{\partial}{\partial t} - \nu\Delta\right)\underline{u}(\underline{x},t) = \underline{L}(\underline{x},t) - \underline{grad}(\alpha) \tag{1}$$

where $\underline{L}$ is the Lamb vector and $\underline{\omega}$ is the vorticity field:

$$\underline{L}(\underline{x},t) = \underline{u}(\underline{x},t) \wedge \underline{\omega}(\underline{x},t) \tag{2}$$

$$\underline{\omega}(\underline{x},t) = \underline{curl}(\underline{u}(\underline{x},t)) \tag{3}$$

with the associated incompressibility condition:

$$div(\underline{u}(\underline{x},t)) = 0\ . \tag{4}$$

The curl of Bernoulli's equation (Eq.1) corresponds to the well known vorticity equation:

$$\left(\frac{\partial}{\partial t} - \nu\Delta\right)\underline{\omega}(\underline{x},t) = [\underline{\omega}(\underline{x},t), \underline{u}(\underline{x},t)] \tag{5}$$

the Lie bracket ([.,.]), i.e. a skew product, being then defined as:

$$[X,Y] = \underline{Y} \cdot \underline{\underline{grad}}(\underline{X}) - \underline{X} \cdot \underline{\underline{grad}}(\underline{Y}) \tag{6}$$

The similarity pointed out by Arnold [1] is between the vorticity equation (Eq.5) and Euler's gyroscope equation (Eq.27, see Appendix A). In the perspective of this similarity, the vorticity and the velocity are respectively the analogues of the angular momentum ($\underline{M}$) and of the rotation ($\underline{\Omega}$), the field analogue of the inertial tensor, is the $\underline{curl}$. However, there is a first fundamental difference between their respective Lie algebra. Indeed, while the Lie algebra corresponding to Euler's gyroscope ($so(3)$), associated to the Lie group of rotations in the three-dimensional space ($SO(3)$), is finite (since it can be defined as the set of three dimensional vectors ($\Re^3$) with the vector product (see Appendix A)), the Lie algebra corresponding to the vorticity equation (on a sub-set D of $\Re^3$) is infinite. Indeed, the latter can be defined as being the set of divergence-free vector fields and it is associated to the group (being noted SDiff D by Arnold) of the one-to-one volume preserving transformations of D.

Both are obviously infinite [a]. The infinite dimensionality is not only related to the intervention of partial instead of ordinary differentiations, as well as the field nature of the velocity, but fundamentally to the phenomenology of fully developed turbulence. Indeed, an infinite number of degrees of freedom should intervene when considering the singular limit of the viscosity going to zero (or correspondingly the Reynolds number going to infinity): one expects the development of a spectrum similar to Kolmogorov-Obukhov spectrum [5,6] down to a viscous scale going to zero, i.e. a number of scales [b] going to infinity. A linear drag can be introduced into Euler's gyroscope equation (Eq.27) in analogy to the viscous term of Navier-Stokes equation (Eq.1). However, the singular perturbation corresponding to the latter has a global effect by creating a flow of energy (respectively of enstrophy) down to smaller scales in 3-D turbulence (respectively 2-D turbulence), although it intervenes *directly* only in the viscous range. This fundamental scale problem clearly points out the necessity of dealing with an infinite dimensional Lie algebra. As shown in the following sections, it rather involves an infinite hierarchy of gyroscopes than being analogous to one of them. Furthermore, even for a finite number of modes, the Lie bracket (Eq.6) defined by the vorticity equation (Eq.3) does not correspond to the vector product. It is not dimensionless and introduces therefore a scale dependency. However, it is relevant for the 2-D turbulence, but in a new context (Sect.5).

3 Scaling Gyroscopes Cascade for 3-D turbulence

For 3-D turbulence a rather opposite analogy is considered: the velocity, the vorticity, the energy and the helicity are respectively the analogues of the angular momentum ($\underline{M}$), of the angular velocity ($\underline{\Omega}$), of the square of the momentum (M^2) and of the energy ($\underline{M} \cdot \underline{\Omega}$). This analogy can be better appreciated when one considers interactions which yield a divergence-less Lamb vector. Indeed, the pressure gradient does not intervene any longer (since it is only needed to enforce incompressibility) in the r.h.s. of the Bernoulli's equation (Eqs.1-3) which is therefore analogue to the Euler's equation (Eq.27):

$$\left(\frac{\partial}{\partial t} - \nu\Delta\right)\underline{u}(\underline{x},t) = \underline{u}(\underline{x},t) \wedge \underline{\omega}(\underline{x},t) \tag{7}$$

[a] It might be important to note that the intrinsic dimensions of the algebra or groups, are not to be confused with the dimension of one of the space on which act one of their representations. Indeed, the latter could be infinite even in the case of a finite algebra.

[b] However, as discussed in the next section, the number of degrees of freedom is larger than the number of scales.

More generally, one may introduce in the Bernoulli's equation (Eq.1) instead of the pressure gradient the projector $\underline{\underline{P}}(\underline{\nabla})$ (resp. $\underline{\underline{\widehat{P}}}(\underline{k})$ in Fourier space, where $\widehat{.}$ denotes the Fourier transform) on divergence-free vector fields :

$$P_{i,j}(\underline{\nabla}) = \delta_{i,j} - \nabla_i \nabla_j \Delta^{-1} \; ; \quad \widehat{P}_{i,j}(\underline{k}) = \delta_{i,j} - k_i k_j / k^2 \tag{8}$$

which yields[c] an expression (either in physical space or in Fourier space) rather similar to Euler equations of a rigid body motion (Eq.27):

$$\left(\frac{\partial}{\partial t} - \nu\Delta\right) \underline{u}(\underline{x},t) = \underline{\underline{P}}(\underline{\nabla}) \cdot \underline{u}(\underline{x},t) \wedge \underline{\omega}(\underline{x},t) \tag{9}$$

$$\left(\frac{\partial}{\partial t} + \nu k^2\right) \underline{\widehat{u}}(\underline{k},t) = \underline{\underline{\widehat{P}}}(\underline{k}) \cdot \int_{\underline{p}+\underline{q}=\underline{k}} \underline{\widehat{u}}(\underline{p},t) \wedge \underline{\widehat{\omega}}(\underline{q},t) d\underline{p} \tag{10}$$

The projector $\underline{\underline{\widehat{P}}}(\underline{k})$ corresponds to the velocity-vorticity vertex of interactions for a triad of wave vectors $(\underline{k},\underline{p},\underline{q})$ maintaining merely the orthogonality condition corresponding to incompressibility (Eq.4):

$$\underline{k} \cdot \underline{\widehat{u}}(\underline{k},t) = 0 \tag{11}$$

it has the advantage to be dimensionless. In a general manner, Navier-Stokes equations (in the Fourier space) correpond to an infinite sum of gyroscope-type equations. The (complex) analogues of $\underline{M}$ and $\underline{\Omega}$ being respectively the triplet $(\underline{u}(\underline{k}),\underline{u}(\underline{p}),\underline{u}(\underline{q}))$ and $(\underline{\omega}(\underline{k}),\underline{\omega}(\underline{p}),\underline{\omega}(\underline{q}))$ of a triad $(\underline{k}+\underline{p})+\underline{q}=\underline{0})$ of direct interaction, the Lie bracket being the vector product modulated by the projector $\underline{\underline{\widehat{P}}}(\underline{k})$. However, this projector reduces[4] at first order to the identity for nonlocal direct[7] interactions ($max(\underline{k},\underline{p},\underline{q}) \geq \lambda min(\underline{k},\underline{p},\underline{q})$, λ being the arbitrary nonlocalness parameter) which satisfy some orthogonal conditions ($\{|\underline{k}| \ll |\underline{p}| \approx |\underline{q}|$ and $\underline{p} \perp \underline{k}\}$ and $\{|\underline{p}| \ll |\underline{k}| \approx |\underline{q}|$ and $\underline{\widehat{u}}(\underline{p}) \| \underline{k}\}$). Corresponding to Eq.7, it yields the following nonlocal orthogonal approximation of Eq.10:

$$\left(\frac{\partial}{\partial t} + \nu k^2\right) \underline{\widehat{u}}(\underline{k}) = \int_{|\underline{p}| \geq \lambda |\underline{k}|} \underline{\widehat{u}}(\underline{p}) \wedge \overline{\underline{\widehat{\omega}}}(\underline{p}) d^d\underline{p} + \left(\int_{|\underline{p}| \leq \lambda^{-1}|\underline{k}|} \underline{\widehat{u}}(\underline{p}) d^d\underline{p}\right) \wedge \underline{\widehat{\omega}}(\underline{k}) \tag{12}$$

where the overline denotes the complex conjugate.

[c] Indeed $\underline{\underline{P}}(\underline{\nabla})(\underline{u}) = \underline{u}$ and $\underline{\underline{P}}(\underline{\nabla})(\underline{grad}(\alpha)) = \underline{0}$.

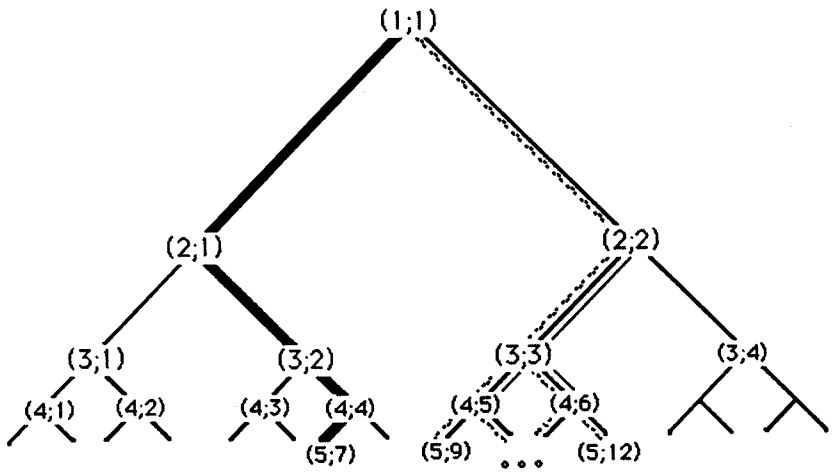

Figure 1: Scheme of a discrete Scaling Gyroscope Cascade model. In this one dimensional cut, each eddy is daughter of a larger scale eddy and mother of two smaller scale eddies. The light thin line indicates interactions for eddy (3;3) in 3-D turbulence, whereas the dashed line indicates its interactions in 2-D turbulence. The thick line points out one of possible most energetic paths, therefore a possible reduction to a shell-model.

4 Discrete SGC models

The discretization of Eq.12 poses interesting problems. One very crude way of doing it corresponds to reduce it to a scalar equation, i.e. to reduce the vector model to a so-called "shell-model"[8,9], by estimating an averaged characteristic velocity shear u_n (with corresponding vorticity $k_n u_n$) on shells of wave-vectors $|\underline{k}| \approx k_n$, the wave-number k_n being the inverse of scale of the corresponding eddies which is dicretized in a exponential way ($l_n = L/\lambda^n$, L being the outer scale). Considering only interactions between successive scales, although considering rather low scale ratio (usually $\lambda = 2$), one can obtain the following:

$$\left(\frac{d}{dt} + \nu k_n^2\right) u_n = k_n u_n u_{n-1} - k_{n+1} u_{n+1}^2 \tag{13}$$

by an over simplification of a more complete model. The latter is indeed needed since the space dimension is absent in Eq.13, whereas it is crucial for the development of intermittency. The relevance of this drastic reduction was already questionned[4,10], as well as the relevance of models having a number of

eddies which do not increase algebraically with the inverse of the scale [d] (e.g. a number independent of the scale [11]). In order to take into account the space dimension, while keeping an exponential discretization of scales (which is not manageable with Fourier transform), it suffices to introduce a tree structure of eddies: each eddy having $N(\lambda) = \lambda^D$ sub-eddies which location is labeled by (i) (in correspondence to its center $\underline{x}_n^i$, the distance between two neighboring centers being of the order of l_n). This type of space and scale analysis has been widely used for phenomenological cascade models and is indeed a predecessor of orthogonal wavelets decomposition [12]. To the eddy of size l_n and a location $\underline{x}_n^i$ corresponds a velocity field $(\underline{\widehat{u}}_n^i)$ and vorticity field $(\underline{\widehat{\omega}}_n^i)$ Fourier/wavelet components, as well as the corresponding wave-vector $(\underline{k}_n^i)$:

$$\underline{\widehat{u}}_n^i \equiv \underline{\widehat{u}}(\underline{k}_n^i) \; ; \quad \underline{\widehat{\omega}}_n^i = i\underline{k}_n^i \wedge \underline{\widehat{u}}_n^i \; ; \quad k_n = |\underline{k}_n^i| \tag{14}$$

For simplicity sake of numerical simulations, we will restrict our attention to one dimensional cuts [e] of 2-D or 3-D turbulence. In the latter case, the tree-structure of interactions is based on the fundamental triads of (direct) interactions $(\underline{k}_{n-1}^i, \underline{k}_n^{2i-1}, \underline{k}_n^{2i})$, between a mother and two daughter eddies $(i = \overline{1, 2^{n-1}})$, whereas it is more involved for the former (see Fig.1 and Sect.5). For 3-D turbulence, one obtains [4] the following equation of evolution (omitting temporarily the interactions outside of the triad $(\underline{k}_{n-1}^i, \underline{k}_n^{2i-1}, \underline{k}_n^{2i})$ as well as the viscous term) for the analogues of the momentum $(\underline{M})$ and of angular velocity $(\underline{\Omega})$:

$$\frac{d\underline{M}_{n-1}^i}{dt} = \underline{M}_{n-1}^i \wedge \underline{\Omega}_{n-1}^i \; ; \quad \underline{\Omega}_{n-1}^i = \underline{\underline{J}}_{n-1}^i \cdot \underline{M}_{n-1}^i \tag{15}$$

with the following matrix representations:

$$\begin{bmatrix} \widehat{u}_n^{2i} \\ \widehat{u}_{n-1}^i \\ \widehat{u}_n^{2i-1} \end{bmatrix} = i\left[M_{n-1}^i\right] = i \begin{bmatrix} u_n^{2i} \\ u_{n-1}^i \\ u_n^{2i-1} \end{bmatrix} \tag{16}$$

$$\begin{bmatrix} \widehat{\omega}_n^{2i-1} \\ 0 \\ \widehat{\omega}_n^{2i} \end{bmatrix} = \left[\Omega_{n-1}^i\right] = ik_n \begin{bmatrix} \widehat{u}_n^{2i-1} \\ 0 \\ \widehat{u}_n^{2i} \end{bmatrix} \tag{17}$$

[d] Indeed this number $N(\ell)$ should scale as $N(\ell) \sim \ell^{-D}$, where ℓ is the scale and D is the dimension of the model. D can be lower than the dimension of the turbulence itself (e.g. for a D-dimensional cut).

[e] The wave-vectors $\underline{k}_n^i$ do not need to belong to the axis of the cut.

and the analogue $(\underline{\underline{J}}_{n-1}^i)$ of the projection of inverse of the inertia tensor on the triad corresponds to:

$$\underline{\underline{J}}_{n-1}^i = k_n \underline{\underline{K}} \; ; \quad [K] = \begin{bmatrix} 0 & 0 & 1 \\ 0 & 0 & 0 \\ 1 & 0 & 0 \end{bmatrix} \tag{18}$$

The equation of evolution of $\widehat{u}_m^j$ corresponds therefore to the coupling of two equations of gyroscope type (Eq.15), therefore to the following (in general complex) scalar equation of evolution for the velocity amplitude u_m^j of the wave vector $\underline{k}_m^j$:

$$\left(\frac{d}{dt} + \nu k_m^2\right) u_m^j = k_{m+1}\left[|u_{m+1}^{2j-1}|^2 - |u_{m+1}^{2j}|^2\right] + (-1)^j k_m u_m^j u_{m-1}^{a(j)} \tag{19}$$

$a(j)$ being the location index of its "ancestor" $(= E\left(\frac{j+1}{2}\right))$, $E(x)$ being the integer part of the real x $(E(x) \leq x < E(x)+1)$.

The SGC model for 3-D turbulence can be reduced to the shell-model defined by Eq.13, as soon as one observes (as done on a similar model [13]) that at each time there is a most active path on the tree connecting the largest structures to the smallest ones (with a unique eddy at each level) along which most of the energy transfer occurs (see Fig.1). This very crude understanding of intermittency corresponds to eliminate the spatial index j in Eq.19 with the very unfortunate consequence of eliminating the crucial space dimension, as discussed above.

5 The very special case of 2-D turbulence

It is well known that 2-D turbulence is rather peculiar, since it has a family of invariants rather different from the 3-D case (or any extensions for a dimension $d > 2$). This is due to the simple fact that the vorticity $(\underline{\omega})$, as well as the potential vector $(\underline{\Psi})$ of a 2-D flow are orthogonal to the plane of the flow and its velocity, and are therefore defined by their scalar components along the axis perpendicular to the flow:

$$\underline{\omega} = \omega \underline{z} \; ; \quad \underline{\Psi} = \Psi \underline{z} \; ; \quad \omega = -\Delta\Psi \tag{20}$$

Ψ being the current function. This orthogonality introduces some simplifications in the vorticity equation (Eq.5) and its corresponding Lie bracket, (Eq.6):

$$[\underline{\omega}(\underline{x}, t), \underline{u}(\underline{x}, t)] = -\underline{u}(\underline{x}, t) \cdot \underline{\underline{grad}}(\underline{\omega}(\underline{x}, t)) \tag{21}$$

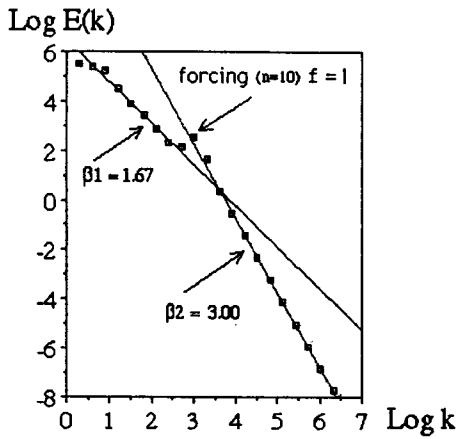

Figure 2: The energy spectrum (averaged over 1024 realizations) of the SGC for 2-D turbulence (forcing at level $n = 10$) displays an inverse energy cascade for low wave numbers (levels $n < 10$) with an algebraic slope close to $\beta_1 = 1.67$, as well as a direct cascade of enstrophy for high wave numbers (levels $n > 10$), with a slope close to $\beta_2 = 3.0$. Logs are base 10.

there is only advection, the stretching term $(\underline{\omega} \cdot \underline{\underline{grad}}(\underline{u}))$ being strictly zero. This introduces the enstrophy (ω^2) as a second quadratic invariant, whereas helicity $(\underline{\omega} \cdot \underline{u})$ is strictly zero. The Fourier transform of the vorticity equation:

$$\left(\frac{\partial}{\partial t} + \nu k^2\right) \widehat{\omega}(\underline{k}, t) = \int_{\underline{p}+\underline{q}=\underline{k}} d^2\underline{p} \ [\Psi(\underline{p}), \omega(\underline{q})] \tag{22}$$

makes intervene the following Lie bracket ((.,.,.) denoting the mixed product):

$$[\Psi(\underline{p}), \omega(\underline{q})] = \frac{1}{2}(\underline{q}, \underline{p}, \underline{z}) \left(\widehat{\Psi}(\underline{p})\widehat{\omega}(\underline{q}) - \widehat{\omega}(\underline{p})\widehat{\Psi}(\underline{q})\right) \tag{23}$$

and corresponds to an infinite sum of gyroscope-type equations. The (complex) analogues of $\underline{M}$ and $\underline{\Omega}$ being respectively the vectors $(\omega(\underline{k}), \omega(\underline{p}), \omega(\underline{q}))$ and $(\Psi(\underline{k}), \Psi(\underline{p}), \Psi(\underline{q}))$ of a triad $(\underline{k} + \underline{p}) + \underline{q} = \underline{0})$ of direct interaction. The enstrophy is therefore the anologue of the square of the momentum, whereas the (turbulent) energy is the analogue of the energy of the gyroscope. The Laplacian is the analogue of the inverse of the inertial tensor.

The first order approximation used for discretization of the 3-D case cancels since the Lie bracket (Eq.23) is strictly zero for any interaction triad having

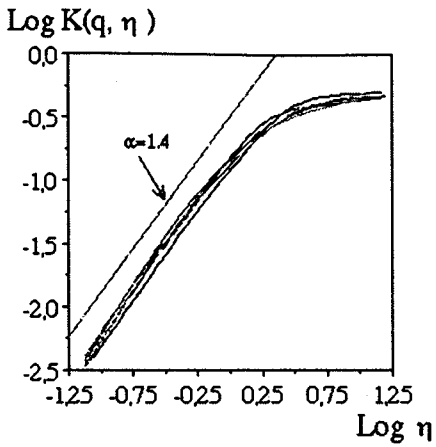

Figure 3: Log of the scaling exponent $(K(q,\eta))$ vs. Logη $(\eta \in (0.3; 3))$ of the spatial flux of energy at medium levels (i.e. 5, 6 and 7) of 2-D SGC (32 levels) and 3-D SGC (19 levels) with the fixed order of moment $q = 1.3$. The different curves are indistinguishable and yield the same estimates: $\alpha \approx 1.4 \pm 0.05$ (the slope of the curves) and $C_1 \approx 0.25 \pm 0.05$ (the intercept with the vertical axis).

two parallel wave-vectors. One has therefore to consider a second order approximation: instead of considering direct interactions between eddies of two successive levels (mother and daughters), one has to consider interactions between three successive levels (mother, daughter and grand-daughter). This implies (see Fig.1) that direct interactions links a given level (m) of the cascade to the two previous ones $(m-1,\ m-2)$ as well as to the two following ones $(m+1,\ m+2)$. This yields an algebra more involved than for the case of 3-D turbulence (Eq.19) and which is generated by commutators of $\widehat{\Psi}$ and $\widehat{\omega}$:

$$C^{i,i'}_{n,n'} = (\underline{q}^{i'}_{n'}, \underline{p}^{i}_{n}, \underline{z})[\Psi(\underline{p}^{i}_{n}), \omega(\underline{q}^{i'}_{n'})]$$

$$\left(\tfrac{\partial}{\partial t} + \nu k^2_m\right) \widehat{\omega}^j_m = C^{a(j),a(a(j))}_{m-1,m-2} + \textstyle\sum_{d(j)=2^{2j-1},2^{2j}} (C^{d(j),a(j)}_{m+1,m-1} \tag{24}$$

$$+ \textstyle\sum_{d^2(j)=2^{4j-2},2^{4j}} C^{d^2(j),d(j)}_{m+2,m})$$

The analogues of the energy and of the square of angular momentum are indeed invariant, since we have the detailed conservation laws (similar to Eq.32)

for any triad $((\underline{k},\underline{p},\underline{q});\ \underline{k}+\underline{p}+\underline{q}=\underline{0})$:

$$[\Psi(\underline{p}),\omega(\underline{q})]\Psi(\underline{k})+[\Psi(\underline{q}),\omega(\underline{k})]\Psi(\underline{p})+[\Psi(\underline{k}),\omega(\underline{p})]\Psi(\underline{q})=0 \qquad (25)$$

$$[\Psi(\underline{p}),\omega(\underline{q})]\omega(\underline{k})+[\Psi(\underline{q}),\omega(\underline{k})]\omega(\underline{p})+[\Psi(\underline{k}),\omega(\underline{p})]\omega(\underline{q})=0 \qquad (26)$$

Due to the existence of these two invariants, SGC yields a spectrum subrange (with slope $-\frac{5}{3}$) which corresponds to an inverse energy cascade as well as spectrum subrange (with slope -3) which corresponds to a direct enstrophy cascade (see Fig.2).

6 SGC models and multifractal analysis

SGC models are fundamentally deterministic contrary to the multiplicative processes [14–22] (see Appendix B for a summary): only the forcing could be stochastic. However, it was checked that the SGC is rather independent[4] of the type of forcing used. Therefore, we used for simulations a constant unit forcing which intervenes only at a given level of the cascade (on the level $n=1$ and on the level $n=10$ for the 3-D case and the 2-D case respectively). Long runs (e.g. 1024 large eddy turn-over times) are easily performed on work stations, using nevertheless a fourth-order Runge-Kutta scheme, for large Reynolds numbers: 32 levels of SGC for 2-D turbulence simulations, in order to exhibit clearly the two scaling subranges; 19 levels of SGC for 3-D turbulence simulations yielding $Re \approx 6\cdot 10^7$.

Spectra of 3-D case simulations display[4] a slope close to the Kolmogorov-Obukhov [5,6] $\beta=-\frac{5}{3}$ which corresponds to the trivial scaling of Eq.19 when assuming a constant flux of energy. Spectra of 2-D case simulations (Fig.2) yield clearly the energy subrange (algebraic slope extremely close to $\beta_1=1.67$) as well as the enstrophy subrange (slope extremely close to $\beta_2=3.0$).

However, spectra do not give direct insights on intermittency. We characterise this intermittency in the framework of universal multifractals. 3-D SGC numerical simulations clearly support[4] strong universality [18, 23] (the misnamed Log-Lévy processes) rather than weak universality (e.g. Log-Poisson statistics [24–27]), only the former possess [28] attractive and stable properties. Log-Lévy statistics of (conservative) fluxes are defined by only two parameters (Appendix B): the mean fractality C_1 and the Lévy index α of multifractality. We estimate (Fig.3) them by a Double Trace Moment (DTM) analysis [29,30] with an order of moment $q=1.5$, starting from the level 7 of 2-D and 3-D SGC simulations. Similar results were obtained with various values of order of moments $q\in(0.8,2)$. These results, $C_1\approx 0.25\pm 0.05$, $\alpha\approx 1.4\pm 0.05$ are extremely close to those obtained for atmospheric turbulence [31,32, 10, 28]. On the contrary, the one-path model or shell model (Eq.13) for 3-D turbulence yields $C_1\approx 0.4\pm 0.05$ and $\alpha\approx 0.6\pm 0.05$. The latter estimate with $\alpha<1$ corresponds to qualitative different behavior of multifractality [33, 34]: singularities are bounded, whereas they are not for $\alpha\geq 1$.

Conclusion

The Scaling Gyroscopes Cascade was derived from rather abstract considerations on the structure of the Navier-Stokes equations: its Lie structure. Nevertheless, it yields concrete dynamical models which can be used to investigate fundamental questions of turbulence. We specifically investigated the questions of multifractal universality for 3-D and 2-D turbulence. Numerical simulations of corresponding SGC yield indistinguishable estimates of the universal parameters (C_1, α) of energy fluxes and confirm the theoretical common value $H=\frac{1}{3}$ for the velocity field. Furthermore, these numerical estimates of C_1 and α are close to different estimates for atmospheric turbulence, in agreement with the strong similarities of structure between SGC and Navier-Stokes equations. On the contrary, we obtained absolutely different class of universality ($\alpha<1$) for the shell-model derived by over-simplifying the SGC.

Acknowledgments

We heartily thank A. Avez, A. Babiano, M. Larcheveque, H.K. Moffatt, A.M. Yaglom for enlightening discussions, F. Schmitt, D. Marsan and C. Naud for helpful comments. Partial support by INTAS 93-1194 grant is acknowledged.

Appendix A: Euler's theorems of a rigid body motion

First Euler's theorem or Euler's equation for a rigid body (attached to a fixed point with no torque), often called the gyroscope equation, is:

$$\frac{d\underline{M}}{dt}=[\underline{M},\underline{\Omega}]\equiv \underline{M}\wedge\underline{\Omega} \qquad (27)$$

where $\underline{M}$ is its angular momentum and $\underline{\Omega}$ its rotation (both relative to the body frame); the Lie bracket being defined by the vector product $\wedge$. The (quadratic) non linearity of the (apparently linear) equation results from the linear relationship between angular momentum and rotation via the (second order) moment of inertia tensor $\underline{\underline{I}}$ or its inverse ($\underline{\underline{J}}=\underline{\underline{I}}^{-1}$), both being symmetric:

$$\underline{M}=\underline{\underline{I}}\cdot\underline{\Omega}\ ;\quad \underline{\Omega}=\underline{\underline{J}}\cdot\underline{M} \qquad (28)$$

Therefore, the gyroscope equation is quadratic in the angular momentum. The equation of motion relative to the body frame (Eq.27) is equivalent to Newton's law of the conservation of angular momentum relative to space (M_s):

$$\frac{dM_s}{dt} = 0 \tag{29}$$

This second Euler's theorem is in fact a particular case of Noether's theorem stating that there is an invariant associated with any equation of motion. There are two associated quadratic invariants to (Eq.27), the first one being the square of the angular momentum (M^2). The second quadratic invariant is the kinetic energy of the body:

$$T = \frac{1}{2}\,\underline{M}\cdot\underline{\Omega} \equiv \frac{1}{2}\,\underline{M}\cdot(\underline{J}\cdot\underline{M}) \tag{30}$$

One may note that the Fourier components of the fields require to consider the rather straightforward extension of complex gyroscopes (complex conjugates being denoted by an overbar):

$$\frac{d\overline{\underline{M}}}{dt} = [\underline{M},\underline{\Omega}] \tag{31}$$

The Hermitian extension of the Euclidean structure preserves the quadratic invariants, since the notion of mixed products (denoted by $(.,.,.)$) is unchanged:

$$\frac{dT}{dt} = \Re(\underline{M},\underline{\Omega},\underline{\Omega}) \equiv 0\ ; \qquad \frac{dM^2}{dt} = 2\Re(\underline{M},\underline{\Omega},\underline{M}) \equiv 0 \tag{32}$$

Appendix B: Multifractal processes and universality

In a stochastic multiplicative process $\varepsilon(\underline{x},t)$, the successive cascade steps define the random fraction of the flux transmitted to smaller scales and they create an infinite hierarchy of singularities γ, i.e. at any scale resolution $\lambda = L/\ell$ (L being the outer scale, ℓ the scale of observation):

$$\varepsilon_\lambda \approx \lambda^{\gamma'}\varepsilon_1\ ; \qquad \Pr(\gamma' \geq \gamma) \approx \lambda^{-c(\gamma)} \tag{33}$$

where "Pr" indicates "probability", $c(\gamma)$ is the codimension/Cramer function [18, 20, 33, 35]. $\gamma > 0$ is indeed the algebraic order of divergence of $\varepsilon_\lambda(\underline{x},t)$; $\lambda \to \infty$. It is equivalent (by the Mellin transform) to consider the scaling of the different orders (q) of moments with the associated scaling moment functions $K(q)$:

$$< (\varepsilon_\lambda)^q > \approx \lambda^{K(q)} \tag{34}$$

where the angle brackets indicate ensemble averages. In fact, $c(\gamma)$ and $K(q)$ are simply related by the Legendre transform [36].

The only general constraints on the two functions $c(\gamma)$ and $K(q)$ are that they should be both convex, and $c(\gamma)$ should be an increasing function. However, due to the existence of stable and attractive multifractal processes under rather general circumstances, mixing of different multifractal processes may lead to universal processes [18,33] which depend on very few aspects of the initial processes. Indeed - up to a critical order [37,38] q_D - these universal multifractal processes have codimension and moments scaling functions ruled by only three fundamental exponents:

- The Hurst exponent H measures the degree of non conservation of the mean field: $< \varepsilon_\lambda > \approx \lambda^{-H}$. $H = 0$ for conservative fields (e.g. the energy flux).
- The mean fractality C_1 measures the fractality/sparseness of the mean field, it corresponds at the same time to the codimension and the singularity of the mean field.
- The Lévy index α ($\alpha \in (0;2]$) determines the extent of multifractality, it is indeed the Lévy index of the generator of the process.

Double Trace Moment (DTM) analysis [29,30] is rather convenient in order to estimate the mean singularity C_1 and the Lévy index α of a conservative multifractal field. It considers in fact the scaling function $K(q,\eta)$ ($K(q,1) \equiv K(q)$) of the normalized η power of the field [37] ($\epsilon_\lambda^{(\eta)} = \frac{\epsilon_\lambda^\eta}{\langle\epsilon_\lambda^\eta\rangle}$). For (strong) universal multifractals: $K(q,\eta) = \eta^\alpha K(q)$.

References

1. V.I.Arnold, *Ann. Inst. Fourier (Grenoble)*, **16**, 319 (1966).
2. A.M.Obukhov, *Fluid Dynam. Trans.*, **5**, 193 (1971).
3. H.Lamb, *Hydrodynamics, 6th Ed.*, (Cambridge University Press, Cambridge, 1963).
4. Y.Chigirinskaya and D.Schertzer in *Stochastic Models in Geophysics*, Eds. A.Molchanov and W.A.Woyczynski, (Springer-Verlag, 1996).
5. A.N.Kolmogorov, *Dokl. Acad. Sci. USSR*, **30**, 299 (1941).
6. A.M.Obukhov, *Dokl. Acad. Sci. USSR*, **32**, 22 (1941).
7. D.C.Leslie, *Developments in the theory of turbulence*, (Clarendon Press, Oxford, 1973).
8. E.B.Gledzer, *Izv. Acad. Sci. USSR, MFG*, **1**, (1980).
9. E.B.Gledzer, E.V.Dolzhansky and A.M.Obukhov, *Systems of fluid mechanical type and their application*, (Nauka, Moscow, 1981), (in Russian).
10. Y.Chigirinskaya, D.Schertzer, S.Lovejoy, A.Lazarev and A.Ordanovich, *Nonlinear Processes in Geophysics*, **1**, 105 (1994).

11. S.Grossmann and D.Lohse, *Europhys. Lett.*, **21**, 201 (1993).
12. V.D.Zimin in *Nonlinear Dynamics of Structures*, Eds. R.Z.Sagdeev et al., (World Scientific, Singapore, 1991).
13. A.M.Obukhov and E.V.Dolzhansky, *Geoph. Fluid. Dyn.*, **6**, 195 (1975).
14. A.M.Yaglom, *Sov. Phys. Dokl.*, **2**, 26 (1966).
15. E.A.Novikov and R.Stewart, *Izv. Acad. Sci. USSR*, **3**, 408 (1964).
16. B.Mandelbrot, *J. Fluid Mech.*, **331**, (1974).
17. D.Schertzer and S.Lovejoy in *Turbulence and chaotic phenomena in fluids*, Ed. T.Tatsumi, (North Holland, 1984).
18. D.Schertzer and S.Lovejoy, *J. Geoph. Res.*, **92**, 9693 (1987).
19. C.Meneveau, K.R.Sreenivasan, *Phys. Rev. Lett.*, **59**, 1424 (1987).
20. B.Mandelbrot in *Turbulence and Stochastic Processes*, Eds. J.C.R.Hunt et al., (The Royal Society, London, 1991).
21. U.Frisch in *Turbulence and Stochastic Processes*, Eds. J.C.R.Hunt et al., (The Royal Society, London, 1991).
22. V.G.Gupta, E.C.Waymire, *J. Appl. Meteor.*, **32**, 251 (1993).
23. D.Schertzer and S.Lovejoy, *J. Appl. Meteor.*, (in press).
24. Z.She and E.Leveque, *Phys. Rev. Letters*, **72**, 336 (1994).
25. E.A.Novikov, *Phys. Rev. E*, **50**, R3303 (1994).
26. B.Dubrulle, *Phys. Rev. Letters*, **73**, 959 (1994).
27. Z.She and E.Waymire, *Phys. Rev. Letters*, **74**, 262 (1995).
28. D.Schertzer, S.Lovejoy and F.Schmitt in *Small-scale structures in 3-D hydro and MHD turbulence*, Eds. M.Meneguzzi et al., (Springer-Verlag, Berlin, 1995).
29. D.Lavallée, *Ph.D. thesis*, (McGill University, Montreal, 1991).
30. D.Lavallée, S.Lovejoy, D.Schertzer and Ph.Ladoy, *Fractals in Geography*, Eds. L.De Cola and N.Lam, (Prentice Hall, New York, 1993).
31. F.Schmitt, D.Lavallée, D.Schertzer and S.Lovejoy, *Phys. Rev. Letters*, **68**, 305 (1992).
32. F.Schmitt, D.Schertzer, S.Lovejoy, and Y.Brunet, *Fractals*, **1**, 568 (1993).
33. D.Schertzer and S.Lovejoy, in *Fractals, Physical origins and properties*, Ed. Pietronero, (Plenum Press, London, 1989).
34. D.Schertzer, S.Lovejoy, D.Lavallée, F.Schmitt, in *Nonlinear Dynamics of Structures*, Eds. R.Z.Sagdeev et al., (World Scientific, Singapore, 1991).
35. Y.Oono, *Theor. Phys. Suppl.*, **99**, 165 (1989).
36. G.Parisi and U.Frisch in *Turbulence and predictability in geophysical fluid dynamics and climate dynamics*, Eds. M.Ghil et al., (N. Holland, 1985).
37. D.Schertzer and S.Lovejoy in *Fractals in the Natural and Applied Sciences*, Ed. M.M.Novak, (North Holland, 1994).
38. D.Schertzer and S.Lovejoy, *Phys. Rep.*, (in press).

Characterisation of Strange Attractors in the Self–Ignition of Coal Stockpiles

G. Continillo, G. Galiero
Istituto di Ricerche sulla Combustione CNR
Via Diocleziano 328 – 80124 Naples, Italy
http://www.irc.na.cnr.it/gc/lab.html

P. L. Maffettone, S. Crescitelli
Dipartimento di Ingegneria Chimica
Università di Napoli "Federico II", Naples, Italy

In previous works, clues of chaotic behaviour were found, by means of numerical experiments, for two distributed–parameter (one– and two–dimensional) models of the self–ignition of coal stockpiles, which incorporated heat conduction, mass diffusion, natural convection, and a one–step Arrhenius exothermic chemical reaction. In this work we characterise quantitatively the strange attractors found. This aim is reached by estimating for each attractor the power spectrum, the Lyapunov Characteristic Exponents (LCE) and the fractal dimension. The Lyapunov exponents are computed by discretising the PDE model along the space coordinate(s), thus generating a model described by a large set of ODEs. The ODEs to be solved for the computation of only the largest LCE are, respectively, 100 and 1250 for the one–dimensional and two–dimensional problem. The algorithm was implemented with MATLAB, SIMULINK, and with a Fortran-C code in the search for the best computational efficiency. The power spectra and the fractal dimensions are computed *a posteriori* by taking, as starting point, time–series generated by numerical simulations. Fractal dimensions are computed using the "Grassberger–Procaccia" algorithm and power spectra are estimated using an FFT algorithm on preprocessed time–series. As a result of systematic explorations, bifurcations and regions of chaotic behaviour are identified in a subset of the parameter space. In this range, even quasi–periodic behaviour has been detected.

1 Introduction

The problem of spontaneous ignition of coal stockpiles is certainly challenging both for safety and for its theoretical implications. Recently many models have been proposed to study this phenomenon: Brooks *et al.* [1,2,3] and Salinger *et al.*[4] determined the static conditions for the beginning of the self–ignition of coal stockpiles without taking into account dynamical aspects. To this aim, they neglected coal consumption, that is with no doubts unimportant during the pre–ignition stage, and used steady–state models without accounting for the transient of temperature and oxygen concentration. From these models it is thus impossible to proceed to characterise dynamically the self–ignition.

In previous papers our group [5,6,7,8] has used dynamical models, both one–